p_T-Dependent Particle Number Fluctuations From Principal Component Analyses in Hydrodynamic Simulations of Heavy-Ion Collisions

Fernando G. Gardim,[1,2] Frédérique Grassi,[3] Pedro Ishida,[3] Matthew Luzum,[3] and Jean-Yves Ollitrault[2]

[1] *Instituto de Ciência e Tecnologia, Universidade Federal de Alfenas, 37715-400 Poços de Caldas, MG, Brazil*
[2] *Institut de physique théorique, Université Paris Saclay, CNRS, CEA, F-91191 Gif-sur-Yvette, France*
[3] *Instituto de Física, Universidade de São Paulo, R. do Matão 1371, 05508-090 São Paulo, SP, Brazil*

We carry out a principal component analysis of fluctuations in a hydrodynamic simulation of heavy-ion collisions, and compare with experimental data from the CMS collaboration. The leading and subleading principal components of elliptic and triangular flow reproduce the trends seen in data. By contrast, the principal components of multiplicity fluctuations show an interesting difference in their p_T dependence for simulations compared to experimental data. Specifically, the leading component increases with p_T in hydrodynamics, while it is constant in experiment. In order to understand how the leading and subleading modes arise, we construct a toy model where the principal components have a simple analytic form. We show how the PCA components depend on fluctuations of the average transverse momentum and of the total multiplicity, as well as correlations between the two, and we verify that hydrodynamic simulations agree with the predictions of the toy model. The difference in the momentum trend is likely due to the fact that hydrodynamic models typically have transverse momentum fluctuations that are larger than seen experimentally.

I. INTRODUCTION

The expansion of the matter formed in nucleus-nucleus collisions at relativistic energies produces a collective transverse flow. This flow is the response to the density gradients in the initial fireball. It is azimuthally asymmetric because the initial fireball is anisotropic and contains hot spots. These inhomogeneities are of interest: they reflect the poorly known mechanism of energy deposition, via the strong interaction, when two nuclei collide, and their influence on the final flow depends on fluid properties, which are also poorly known (e.g. shear and bulk viscosities). A lot of work has been done to relate initial inhomogeneities and final flow of produced particles. In particular the mapping between initial conditions and anisotropic flow has been studied globally and event-by-event [1–6]. To get more detailed information on fluctuations in the initial state, a useful observable is the factorization breaking ratio [7–13], which encodes the correlations of flow harmonics at different transverse momenta or pseudorapidities. More recently a new more precise tool was proposed, the Principal Component Analysis (PCA) for event-by-event fluctuations [14–16] and first experimental results for such an analysis have been presented by the CMS collaboration [17]. The aim of this paper is to present a hydrodynamical study of these observables and point out an interesting difference between data and some hydrodynamic simulations for the $n = 0$ leading and sub-leading components, corresponding to multiplicity fluctuations. These components are sensitive to physics not explored by anisotropic flow and can put new constraints on initial conditions models.

II. PRINCIPAL COMPONENT ANALYSIS

Principal Component Analysis is a common technique for finding patterns in data of high dimension. One tries to find new variables that incorporate as much as possible of the variations. This amounts to diagonalizing the covariance matrix (e.g. [18]). It was first suggested to use it to study event-by-event fluctuations in relativistic nuclear collisions in [14]. For self-consistency, the method is summarized below. Consider a set of collisions or events. For each event, the single particle distribution can be expanded as

$$\frac{dN}{d\vec{p}} = \frac{1}{2\pi}\sum_{n=-\infty}^{+\infty} N(p_T)V_n(p_T)e^{-in\phi} \tag{1}$$

$$= \sum_{n=-\infty}^{+\infty} \mathcal{V}_n(p_T)e^{-in\phi} \tag{2}$$

where $d\vec{p} = dydp_Td\phi$, ϕ is the azimuthal angle of the particle momentum. $\mathcal{V}_n(p_T)$ is a Fourier coefficient (without the usual normalization by multiplicity) which is complex for $n \neq 0$. Its magnitude and orientation vary for each event.

For each transverse momentum bin, the variance can be computed $\langle|\mathcal{V}_n(p_T^a)|^2\rangle - |\langle\mathcal{V}_n(p_T^a)\rangle|^2$ (the average is performed over events) but brings no information about possible relationship between different bins. To investigate how different bins are correlated, one constructs the covariance matrix:

$$\mathcal{V}_{n\Delta}(p_T^a, p_T^b) \equiv \langle\mathcal{V}_n(p_T^a)\mathcal{V}_n^*(p_T^b)\rangle - \langle\mathcal{V}_n(p_T^a)\rangle\langle\mathcal{V}_n^*(p_T^b)\rangle. \tag{3}$$

The terms $\langle\mathcal{V}_n(p_T^a)\rangle$ are zero by azimuthal symmetry, except for $n = 0$.

This covariance matrix is real, symmetric, positive-semidefinite. It can be diagonalized and re-written in

term of its real orthogonal eigenvectors $\mathcal{V}_n^{(\alpha)}(p_T)$

$$\mathcal{V}_{n\Delta}(p_T^a, p_T^b) = \sum_\alpha \mathcal{V}_n^{(\alpha)}(p_T^a)\mathcal{V}_n^{(\alpha)}(p_T^b), \tag{4}$$

from where one can express the flow vector in a given event as

$$\mathcal{V}_n(p_T) = \sum_\alpha \xi_n^{(\alpha)}\mathcal{V}_n^{(\alpha)}(p_T), \tag{5}$$

where $\xi_n^{(\alpha)}$ are coefficients that vary from event to event (specifically, uncorrelated, random complex numbers with zero mean and unit variance). Terms in the right-hand side of Eq. (4) are ordered according to the magnitude of the eigenvalues. Even by truncating the sum to the first two or three terms, one typically obtains a very good approximation to the left-hand side. The largest component $\mathcal{V}_n^{(1)}(p_T)$ is called the leading mode, $\mathcal{V}_n^{(2)}(p_T)$ the sub-leading mode, etc. For comparison with standard flow, it is useful to introduce the following scaled principal components

$$v_n^{(\alpha)}(p_T) = \frac{\mathcal{V}_n^{(\alpha)}(p_T)}{\langle \mathcal{V}_0(p_T)\rangle}. \tag{6}$$

Once the dominant terms in Eq. (4) are determined (i.e. patterns are found in our high dimension data), the physical meaning of these terms must be investigated. This was done in [14–16, 19, 20] and is discussed in section III ($n = 2, 3$) and IV ($n = 0$).

III. RESULTS FOR ANISOTROPIC FLOW

In this section and the next, we present results obtained from a hydrodynamic simulation for a perfect fluid expanding in 3+1 dimensions starting from NeXus initial conditions [21]. The code used, NeXSPheRIO, has been shown to lead to a consistent description of many flow data at top RHIC energies [22–29].

We also have some data accumulated for two centrality windows (0-5 and 20-30%) at $\sqrt{s} = 2.76$ TeV and their compatibility with flow observables more subtly related to fluctuations (scaled harmonic flow distributions, factorization breaking ratio) has been tested [30]. This code is therefore an interesting tool for a first investigation of the PCA results obtained recently by CMS at the LHC [17].

For n=2–3, we show the first two scaled principal components and comparison with CMS data in Fig. 1. Our cuts are $|\eta| < 2.5$ (equivalent to CMS) but $p_T > 0.5$ GeV, slightly higher than CMS $p_T > 0.3$ GeV. We used similar p_T bins as experimentally.

The leading component is straightforward to interpret [14–16]. If it dominates, Eq. (4) yields $\mathcal{V}_{n\Delta}(p_T^a, p_T^b) \sim \mathcal{V}_n^{(1)}(p_T^a)\mathcal{V}_n^{(1)}(p_T^b)$ i.e. there is flow factorization. The event flow defined by Eq. (5) reduces to $\mathcal{V}_n(p_T) \sim \xi_n^{(1)}(p_T)\mathcal{V}_n^{(1)}(p_T)$, i.e., the leading component corresponds to usual anisotropic flow. We have checked explicitly that this is the case (not shown). Concentrating on the region from 0 to 2 GeV, we see that our hydro simulation slightly overestimates the leading components. Inclusion of viscosity would damp them and improve agreement with data, as explicitly shown for the p_T-integrated $n = 3$ leading component in Ref. [15].

Higher-order principal components encode the information about the momentum dependence of flow fluctuations. In this context, it is customary to introduce the factorization breaking ratio

$$r_n = \frac{\mathcal{V}_{n\Delta}(p_T^a, p_T^b)}{\sqrt{|\mathcal{V}_{n\Delta}(p_T^a)|^2|\mathcal{V}_{n\Delta}(p_T^b)|^2}}, \tag{7}$$

which drops below unity in the presence of p_T-dependent flow fluctuations. Note that the numerator and the denominator involve all the principal components, according to Eq. (4). In practice, however, as in [16], we have checked that the first three principal components give a very good approximation of r_n (not shown). The individual principal components express the information contained in the factorization ratio in a simpler way because they are functions of a single variable p_T^a, while r_n is a function of two variables p_T^a and p_T^b. In the range 0 to 2 GeV, the simulations for the scaled sub-leading component capture the main features of the data (the sub-leading component is perpendicular to the leading one, the slightly higher p_T cut should shift the point where it crosses the horizontal axis a little to the right). In [15], it was shown that the p_T integrated scaled sub-leading component for n=3 depends less on viscosity than the leading one.

IV. RESULTS FOR MULTIPLICITIES

We now discuss multiplicity fluctuations, corresponding to $n = 0$ principal components. The comparison between our results and CMS data is displayed in the top panels of Fig. 2. There is rough overall agreement, but not as good as in Fig. 1. The leading component is rather independent of p_T in experiment, while it increases with p_T in our hydrodynamic calculation. The same increase is not seen at RHIC energies (bottom panel of Fig. 2). The increase at LHC energies is not specific to our implementation, as it has been seen by other groups [16, 31]. Such qualitative disagreement between hydrodynamics and experimental data is rare, therefore, we investigate its origin in detail.[1]

In order to understand the principal components for $n = 0$, we introduce a toy model where the fluctuation of

[1] Note that the transport model AMPT without hydrodynamics predicts a flat leading component, as seen in data.

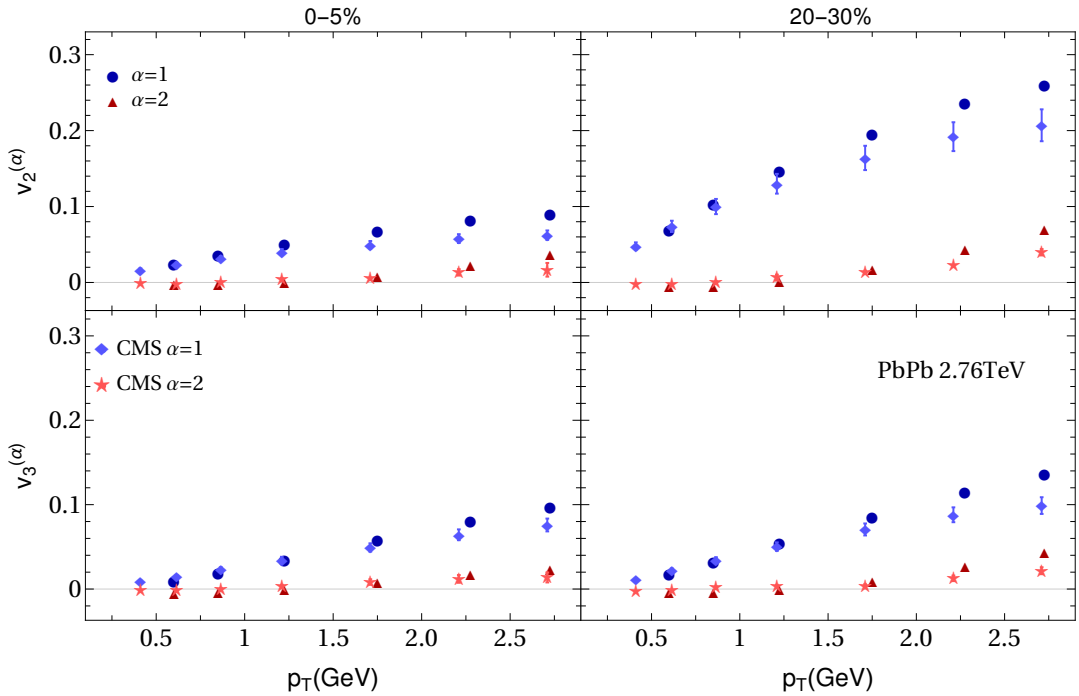

FIG. 1. First two scaled principal components from the ideal fluid calculation in two centrality windows corresponding to central (left) and midcentral (right) collisions. Top: elliptic flow ($n = 2$). Bottom: triangular flow ($n = 3$). Experimental data are from the CMS collaboration [17] (n=2,3).

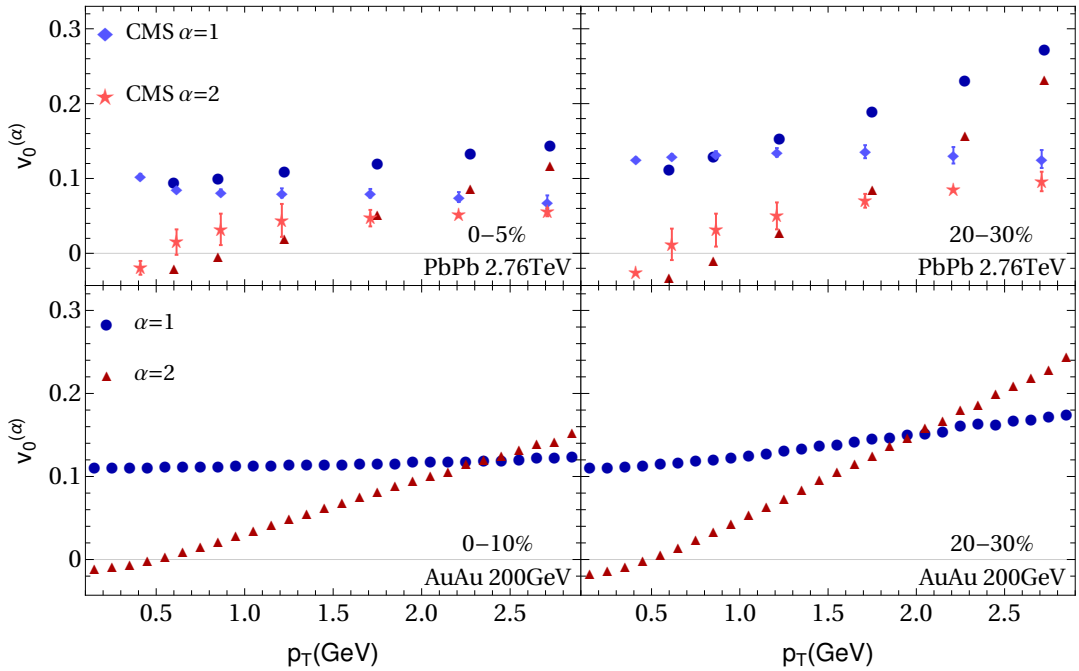

FIG. 2. First two scaled principal components for $n = 0$ (multiplicity fluctuations). The top panels display a comparison between our ideal fluid calculation and CMS data [17], as in Fig. 1. The bottom panels display our predictions for Au+Au collisions at 200 GeV in two centrality windows.

the multiplicity in a p_T bin originates from two sources: 1) fluctuations of the total multiplicity N. 2) fluctuations of the mean transverse momentum $\bar{p}_T$. In addition, we assume for simplicity that the p_T spectrum is exponential:

$$\frac{1}{2\pi}\frac{dN}{dydp_T} = \mathcal{V}_0(p_T) = \frac{2p_T N}{\pi \bar{p}_T^2} e^{-\frac{2p_T}{\bar{p}_T}} \tag{8}$$

where N is the total multiplicity per unit rapidity and $\bar{p}_T$ is the mean transverse momentum in one event. Next, we allow N and $\bar{p}_T$ in a given event to deviate from the event-averaged total multiplicity $\langle N\rangle$, and the event-averaged mean transverse momentum $\langle \bar{p}_T\rangle$ in a centrality bin, respectively:

$$N = \langle N\rangle + \delta N, \tag{9}$$

$$\bar{p}_T = \langle \bar{p}_T\rangle + \delta \bar{p}_T. \tag{10}$$

Expanding Eq. (8) to first order in δN and $\delta\bar{p}_T$, one obtains:

$$\frac{\delta\mathcal{V}_0(p_T)}{\langle \mathcal{V}_0(p_T)\rangle} = \frac{\delta N}{\langle N\rangle} - 2\frac{\delta\bar{p}_T}{\langle\bar{p}_T\rangle} + 2\frac{p_T\delta\bar{p}_T}{\langle\bar{p}_T\rangle^2}. \tag{11}$$

The covariance (3) is then given by

$$\mathcal{V}_{0\Delta}(p_T^a, p_T^b) \equiv \langle \delta\mathcal{V}_0(p_T^a)\delta\mathcal{V}_0(p_T^b)\rangle, \tag{12}$$

where angular brackets denote an average over events in a centrality bin. Inserting Eq. (11) into Eq. (12), one obtains:

$$\begin{aligned}\frac{\mathcal{V}_{0\Delta}(p_T^a, p_T^b)}{\langle \mathcal{V}_0(p_T^a)\rangle\langle \mathcal{V}_0(p_T^b)\rangle} &= \frac{\sigma_N^2}{\langle N\rangle^2} + 4\frac{\sigma_{p_T}^2}{\langle\bar{p}_T\rangle^2} - 4\frac{\langle\delta N\delta\bar{p}_T\rangle}{\langle N\rangle\langle\bar{p}_T\rangle} \\ &+2\left(\frac{\langle\delta N\delta p_T\rangle}{\langle N\rangle\langle\bar{p}_T\rangle} - 2\frac{\sigma_{p_T}^2}{\langle\bar{p}_T\rangle^2}\right)\frac{p_T^a + p_T^b}{\langle\bar{p}_T\rangle} \\ &+4\frac{\sigma_{p_T}^2}{\langle\bar{p}_T\rangle^2}\frac{p_T^a p_T^b}{\langle\bar{p}_T\rangle^2},\end{aligned} \tag{13}$$

where $\sigma_N^2 \equiv \langle\delta N^2\rangle$ and $\sigma_{p_T}^2 \equiv \langle\delta\bar{p}_T^2\rangle$ denote the variance of the multiplicity and mean p_T, respectively. Inspection of the dependence on p_T^a and p_T^b shows that the scaled principal components defined by Eqs. (4) and (6) can only be of the form

$$v_0^{(\alpha)}(p_T) = a^{(\alpha)} + b^{(\alpha)}\frac{p_T}{\langle\bar{p}_T\rangle}, \tag{14}$$

i.e., they are linear in p_T. Since they span a two-dimensional space, this in turn implies that there are at most two principal components (remember that principal components are mutually orthogonal). The full analytic expressions of these principal components are cumbersome. Therefore, we make further simplifying assumptions, by identifying the leading terms in Eq. (13).

Table I gives the values of the relative fluctuations of N and $\bar{p}_T$ in our hydrodynamic calculation, as well as their covariance. The relative fluctuations of N are larger by an order of magnitude, which is explained by the large width of the centrality bin. In the limit where σ_{p_T} and $\langle\delta N\delta\bar{p}_T\rangle$ can be neglected, only the first term remains in the right-hand side of Eq. (13). The covariance matrix trivially factorizes, i.e., there is only one principal component. The scaled principal component, defined by Eq. (6), is:

TABLE I. Values of the variances and covariance of N and $\bar{p}_T$ at LHC and RHIC in our hydrodynamical calculation using NeXSPheRIO.

	$2.76\,TeV$			$200\,GeV$		
centrality	$\frac{\sigma_N}{\langle N\rangle}$	$\frac{\sigma_{p_T}}{\langle\bar{p}_T\rangle}$	$\sqrt{\frac{\langle\delta N\delta\bar{p}_T\rangle}{\langle N\rangle\langle\bar{p}_T\rangle}}$	$\frac{\sigma_N}{\langle N\rangle}$	$\frac{\sigma_{p_T}}{\langle\bar{p}_T\rangle}$	$\sqrt{\frac{\langle\delta N\delta\bar{p}_T\rangle}{\langle N\rangle\langle\bar{p}_T\rangle}}$
0-5 %	0.12	0.026	0.041			
0-10 %				0.11	0.017	0.017
20-30 %	0.16	0.041	0.070	0.12	0.025	0.031

$$v_0^{(1)}(p_T) \simeq \frac{\sigma_N}{\langle N\rangle}. \tag{15}$$

It is independent of p_T. Thus, the fact that our hydrodynamic calculation reproduces the magnitude of $v_0^{(1)}(p_T)$ at low p_T (i.e., for the bulk of produced particles) simply means that it has the correct multiplicity fluctuations. These are largely dominated by the width of the centrality bin used for the analysis, or, equivalently, by impact parameter fluctuations.

We now consider the more general case where $\sigma_{p_T}/\langle\bar{p}_T\rangle$ and $\sqrt{\langle\delta N\delta\bar{p}_T\rangle/\langle N\rangle\langle\bar{p}_T\rangle}$ are not zero, but can still be treated as small quantities. Then, to leading order in these quantities, the scaled principal components are:

$$\begin{aligned}v_0^{(1)}(p_T) &\simeq \frac{\sigma_N}{\langle N\rangle} + \left[\frac{-\left(\frac{\sigma_{p_T}}{\langle\bar{p}_T\rangle}\right)^2 + 2\frac{\langle\delta N\delta p_T\rangle}{\langle N\rangle\langle\bar{p}_T\rangle}}{\left(\frac{\sigma_N}{\langle N\rangle}\right)}\right]\frac{p_T}{\langle\bar{p}_T\rangle}, \\ v_0^{(2)}(p_T) &\simeq -\frac{3}{2}\frac{\sigma_{p_T}}{\langle\bar{p}_T\rangle}\left(1 - \frac{4}{3}\frac{p_T}{\langle\bar{p}_T\rangle}\right).\end{aligned} \tag{16}$$

One can check that with these expressions, the decomposition (4) is satisfied. In terms of the scaled components, this equation can be written:

$$\frac{\mathcal{V}_{0\Delta}(p_T^a, p_T^b)}{\langle \mathcal{V}_0(p_T^a)\rangle\langle \mathcal{V}_0(p_T^b)\rangle} = v_0^{(1)}(p_T^a)v_0^{(1)}(p_T^b) + v_0^{(2)}(p_T^a)v_0^{(2)}(p_T^b). \tag{17}$$

Inserting Eq. (16) into Eq. (17), and expanding to first order in $\langle\delta N\delta\bar{p}_T\rangle$ and $\sigma_{p_T}^2$, one recovers Eq. (13) except for the second and third terms of the first line, which are subleading corrections to the first term.

Equation (16) is a refinement of the zeroth-order result, Eq. (15). A subleading mode $v_0^{(2)}(p_T)$ appears, which is directly proportional to $\sigma_{p_T}/\langle\bar{p}_T\rangle$. The connection between the subleading mode and p_T fluctuations was already made in Ref. [16]. The subleading mode changes sign as a function of p_T, which is imposed by orthogonality with the leading mode. The change of sign occurs at $p_T = (3/4)\langle\bar{p}_T\rangle$, which is rather independent of the centrality, and is in agreement with CMS data.

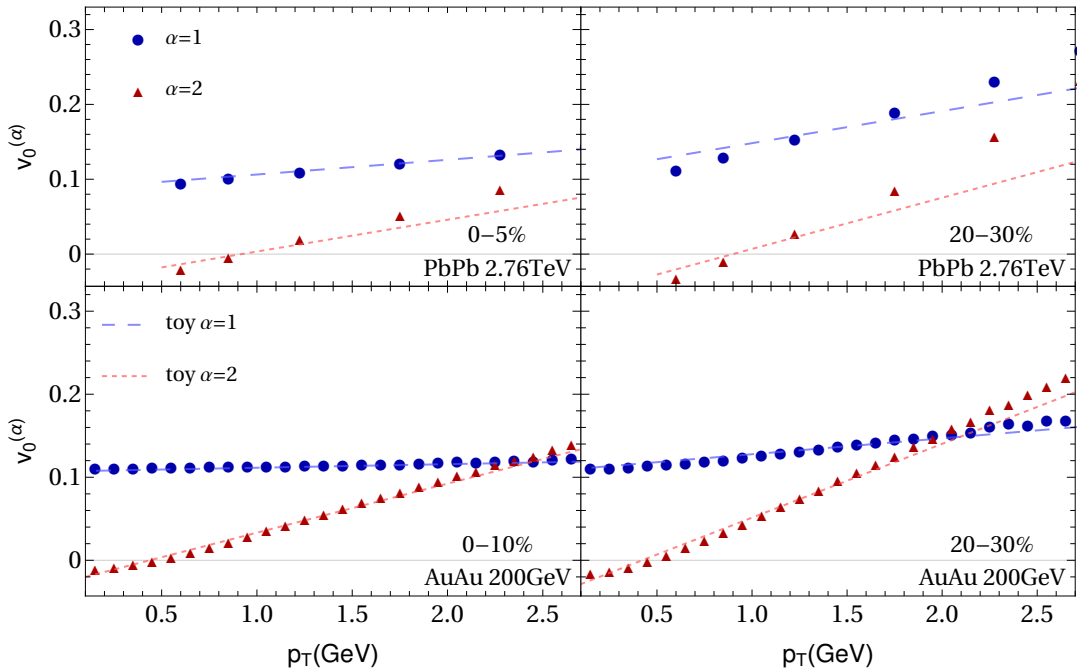

FIG. 3. Comparison between scaled principal components of a full hydrodynamical model (symbols) and the approximate result from the toy model, Eq. (16) (lines). Top: Au+Au collisions at RHIC. Bottom: Pb+Pb collisions at the LHC. As in Figs. 1 and 2, the left panels correspond to central collisions, and the right panels to mid-central collisions.

Figure 3 displays a comparison between Eq. (16) and the result from the full hydrodynamic calculation. Agreement is very good at RHIC and a little worse at LHC (presumably due to the different lower p_T cuts), so one concludes that Eq. (16) captures the physics of the first two $n = 0$ modes.

The motivation for building the toy model was to understand under which condition the leading mode is independent of p_T, or rises with p_T. The first line of Eq. (16) shows that a rise with p_T can be ascribed to a positive correlation between the mean transverse momentum and the multiplicity, represented by the quantity $\langle \delta N \delta \bar{p}_T \rangle$. The fact that this rise is seen in hydrodynamic calculations, not in data, implies that hydrodynamic calculations overestimate $\langle \delta N \delta \bar{p}_T \rangle$. This can be related to the fact that hydrodynamic models yield too large δp_T in general, as pointed out by a study of transverse momentum fluctuations [32]. Since transverse momentum fluctuations in hydrodynamics originate from fluctuations in the transverse size of the interaction region [33], this in turn implies that existing models of initial fluctuations tend to overestimate the size fluctuations.

The conclusion of this study is that a model which predicts the right multiplicity and p_T fluctuations should capture the first two principal components for $n = 0$. The reason why our hydrodynamical model predicts a rise of the leading mode with p_T, which is not seen in data, is that the p_T fluctuations from Table I are too large compared to experimental data from ALICE [38]. The bottom panels of Fig. 2 display our predictions for RHIC. The values of $\sigma_N/\langle N \rangle$ from Table I are comparable with experimental values from PHENIX [36], while the values of $\sigma_{p_T}/\langle \bar{p}_T \rangle$ are slightly too large compared to STAR data [37], but in fair agreement. We therefore expect that our calculation should correctly predict the first two modes of multiplicity fluctuations at RHIC.

V. CONCLUSION

We have compared results from a hydrodynamic simulation using the code NeXSPheRIO with recent experimental data by CMS, on the Principal Component Analysis. The trends for the leading and sub-leading components of elliptic and triangular flow are in fair agreement with data. In contrast, for multiplicity fluctuations, we have pointed out a qualitative disagreement: The leading component increases with p_T in hydrodynamics (here as well as in [16, 31]) while it is constant in data at LHC energies. This has prompted us to analyze this case more thoroughly. We have constructed a toy model which gives result in good agreement with the full hydrodynamic calculation. In this toy model, the subleading component is proportional to the standard deviation of the mean p_T, σ_{p_T}. The leading component is close to $\sigma_N/\langle N \rangle$ at low p_T, but increases with p_T if the fluctuations of p_T are large and correlated with the fluctuations of the multiplicity.

We have thus related $n = 0$ results from the principal component analysis to multiplicity and transverse momentum fluctuations. Fluctuations in N and $\bar{p}_T$ have been attracting attention for a long time because they may probe the QCD phase transition (see e.g. [34]), as well as initial inhomogeneities (see for example [33, 35]). The principal components are sensitive not only to the width of multiplicity and transverse momentum fluctuations, but also to their mutual covariance. They open a new window on initial fluctuations, which can be used to rule out initial condition models.

ACKNOWLEDGMENTS

F.G. acknowledges support from Fundação de Amparo à Pesquisa do Estado de São Paulo (FAPESP grant 2018/18075-0) and Conselho Nacional de Desenvolvimento Científico e Tecnológico (CNPq grant 310141/2016-8). F.G.G. was supported by Conselho Nacional de Desenvolvimento Científico e Tecnológico (CNPq grant 205369/2018-9 and 312932/2018-9) and FAPEMIG (grant APQ-02107-16. P.I. thanks support from Coordenação de Aperfeiçoamento de Pessoal de Nível Superior (CAPES). M.L. acknowledges support from FAPESP projects 2016/24029-6 and 2017/05685-2. F.G., F.G.G. and M.L. acknowledge support from project INCT-FNA Proc. No. 464898/2014-5 and F.G., M.L. and J.-Y.O. from USP-COFECUB (grant Uc Ph 160-16, 2015/13).

[1] F. G. Gardim, F. Grassi, M. Luzum and J. Y. Ollitrault, Phys. Rev. C **85**, 024908 (2012).
[2] F. G. Gardim, J. Noronha-Hostler, M. Luzum and F. Grassi, Phys. Rev. C **91**, no. 3, 034902 (2015).
[3] H. Niemi, G. S. Denicol, H. Holopainen and P. Huovinen, Phys. Rev. C **87**, no. 5, 054901 (2013).
[4] H. Niemi, K. J. Eskola and R. Paatelainen, Phys. Rev. C **93**, no. 2, 024907 (2016).
[5] J. Fu, Phys. Rev. C **92**, no. 2, 024904 (2015).
[6] J. Noronha-Hostler, L. Yan, F. G. Gardim and J. Y. Ollitrault, Phys. Rev. C **93**, no. 1, 014909 (2016).
[7] F. G. Gardim, F. Grassi, M. Luzum and J. Y. Ollitrault, Phys. Rev. C **87**, no. 3, 031901 (2013).
[8] I. Kozlov, M. Luzum, G. Denicol, S. Jeon and C. Gale, arXiv:1405.3976 [nucl-th].
[9] U. Heinz, Z. Qiu and C. Shen, Phys. Rev. C **87**, no. 3, 034913 (2013).
[10] V. Khachatryan *et al.* [CMS Collaboration], Phys. Rev. C **92**, no. 3, 034911 (2015).
[11] F. G. Gardim, F. Grassi, P. Ishida, M. Luzum, P. S. Magalhes and J. Noronha-Hostler, Phys. Rev. C **97**, no. 6, 064919 (2018).
[12] W. Zhao, H. j. Xu and H. Song, Eur. Phys. J. C **77**, no. 9, 645 (2017).
[13] S. McDonald, C. Shen, F. Fillion-Gourdeau, S. Jeon and C. Gale, Phys. Rev. C **95**, no. 6, 064913 (2017).
[14] R. S. Bhalerao, J. Y. Ollitrault, S. Pal and D. Teaney, Phys. Rev. Lett. **114**, no. 15, 152301 (2015).
[15] A. Mazeliauskas and D. Teaney, Phys. Rev. C **91**, no. 4, 044902 (2015).
[16] A. Mazeliauskas and D. Teaney, Phys. Rev. C **93**, no. 2, 024913 (2016).
[17] A. M. Sirunyan *et al.* [CMS Collaboration], Phys. Rev. C **96**, no. 6, 064902 (2017).
[18] J. O. Ramsay and B. W. Silverman, "Functional Data Analysis", Springer, New York-USA (2005).
[19] P. Bozek, Phys. Rev. C **97**, no. 3, 034905 (2018).
[20] Z. Liu, W. Zhao and H. Song, "Principal Component Analysis of collective flow in Relativistic Heavy-Ion Collisions, arXiv:1903.09833
[21] H. J. Drescher, M. Hladik, S. Ostapchenko, T. Pierog and K. Werner, Phys. Rept. **350**, 93 (2001).
[22] W. L. Qian, R. Andrade, F. Grassi, O. Socolowski, Jr., T. Kodama and Y. Hama, Int. J. Mod. Phys. E **16**, 1877 (2007).
[23] R. Andrade, F. Grassi, Y. Hama, T. Kodama and O. Socolowski, Jr., Phys. Rev. Lett. **97**, 202302 (2006).
[24] R. P. G. Andrade, F. Grassi, Y. Hama, T. Kodama and W. L. Qian, Phys. Rev. Lett. **101**, 112301 (2008).
[25] R. P. G. Andrade, A. L. V. R. dos Reis, F. Grassi, Y. Hama, W. L. Qian, T. Kodama and J.-Y. Ollitrault, Acta Phys. Polon. B **40**, 993 (2009).
[26] F. G. Gardim, F. Grassi, Y. Hama, M. Luzum and J. Y. Ollitrault, Phys. Rev. C **83**, 064901 (2011).
[27] F. G. Gardim, F. Grassi, M. Luzum and J. Y. Ollitrault, Phys. Rev. Lett. **109**, 202302 (2012).
[28] J. Takahashi, B. M. Tavares, W. L. Qian, R. Andrade, F. Grassi, Y. Hama, T. Kodama and N. Xu, Phys. Rev. Lett. **103**, 242301 (2009).
[29] W. L. Qian, R. Andrade, F. Gardim, F. Grassi and Y. Hama, Phys. Rev. C **87**, no. 1, 014904 (2013).
[30] L. Barbosa, F. Gardim, F. Grassi, M. Luzum and M. V. Machado, in preparation.
[31] M. Luzum, private communcation about MUSIC code with Trento initial conditions.
[32] P. Bozek and W. Broniowski, Phys. Rev. C **85**, 044910 (2012).
[33] W. Broniowski, M. Chojnacki and L. Obara, Phys. Rev. C **80**, 051902 (2009).
[34] M. Stephanov, J. Phys. Conf. Ser. **27**, 144 (2005).
[35] S. Gavin and G. Moschelli, Phys. Rev. C **85**, 014905 (2012).
[36] A. Adare *et al.* [PHENIX Collaboration], Phys. Rev. C **78**, 044902 (2008).
[37] J. Adams *et al.* [STAR Collaboration], Phys. Rev. C **72**, 044902 (2005).
[38] B. B. Abelev *et al.* [ALICE Collaboration], Eur. Phys. J. C **74**, no. 10, 3077 (2014).